Available online at www.sciencedirect.com
SCIENCE DIRECT®
Biochemical and Biophysical Research Communications 338 (2005) 230–239
BBRC
www.elsevier.com/locate/ybbrc

Review

Post-translational self-hydroxylation: A probe for oxygen activation mechanisms in non-heme iron enzymes ☆

Erik R. Farquhar, Kevin D. Koehntop, Joseph P. Emerson, Lawrence Que Jr. *

Department of Chemistry and Center for Metals in Biocatalysis, University of Minnesota, 207 Pleasant Street SE, Minneapolis, MN 55455, USA

Received 25 August 2005
Available online 2 September 2005

Abstract

Recent years have seen considerable evolution in our understanding of the mechanisms of oxygen activation by non-heme iron enzymes, with high-valent iron-oxo intermediates coming to the forefront as formidably potent oxidants. In the absence of substrate, the generation of vividly colored chromophores deriving from the self-hydroxylation of a nearby aromatic amino acid for a number of these enzymes has afforded an opportunity to discern the conditions under which O_2 activation occurs to generate a high-valent iron intermediate, and has provided a basis for a rigorous mechanistic examination of the oxygenation process. Here, we summarize the current evidence for self-hydroxylation processes in both mononuclear non-heme iron enzymes and in mutant forms of ribonucleotide reductase, and place it within the context of our developing understanding of the oxidative transformations accomplished by non-heme iron centers.

Keywords: Non-heme iron; Oxygen activation; Post-translational modification; Self-hydroxylation; Ribonucleotide reductase; α-Ketoglutarate dependent enzymes

Non-heme iron centers are utilized throughout living systems to activate dioxygen to catalyze a remarkably diverse array of transformations [1–3]. The potential oxidizing power of this class of enzymes is strikingly illustrated by methane monooxygenase (MMOH), which is capable of breaking the high energy C—H bond (104 kcal/mol) in methane to yield methanol [4,5]. This potent reactivity stems from the generation of high-valent iron-oxo intermediates through pathways that involve either a dinuclear or mononuclear iron center (Scheme 1).

For mononuclear non-heme iron enzymes, two distinct pathways are proposed for the generation of the high-valent intermediate (cf. Scheme 1). In the first, associated with the Rieske dioxygenases, binding of O_2 and injection of an electron from a nearby iron–sulfur cluster lead to an iron(III)-peroxo species, and subsequent cleavage of the O—O bond presumably generates an iron(V)-oxo species [2]. This scheme is mechanistically analogous to the generally accepted process in the heme-containing cytochrome P450 enzymes [6,7]. In the second pathway, the iron center utilizes an external cofactor, such as α-ketoglutarate (α-KG) or pterin, to supply two electrons for O_2 reduction. This process generates an iron(IV)-oxo species [8–10], which has recently been shown to be responsible for substrate oxidation in the α-KG dependent enzyme TauD [11].

Diiron non-heme enzymes also share a common oxygen activation process (cf. Scheme 1), which begins with O_2

☆ *Abbreviations:* α-KG, α-ketoglutarate; AlkB, alkylated DNA repair enzyme; ENDOR, electron nuclear double resonance; EPR, electron paramagnetic resonance; ESI-MS, electrospray ionization mass spectrometry; HPPD, 4-hydroxyphenylpyruvate dioxygenase; HppE, (*S*)-2-hydroxypropylphosphonic acid epoxidase, MALDI-TOF, matrix assisted laser desorption ionization-time of flight; MMOH, hydroxylase component of methane monooxygenase; PheH, phenylalanine hydroxylase; PMI, phosphomannose isomerase; R2, the R2 subunit of ribonucleotide reductase; TauD, taurine/α-KG dioxygenase; TfdA, 2,4-dichlorophenoxyacetate/α-KG dioxygenase; TyrH, tyrosine hydroxylase.

* Corresponding author. Fax: +1 612 624 7029.
E-mail address: que@chem.umn.edu (L. Que).

0006-291X/$ - see front matter © 2005 Elsevier Inc. All rights reserved.
doi:10.1016/j.bbrc.2005.08.191

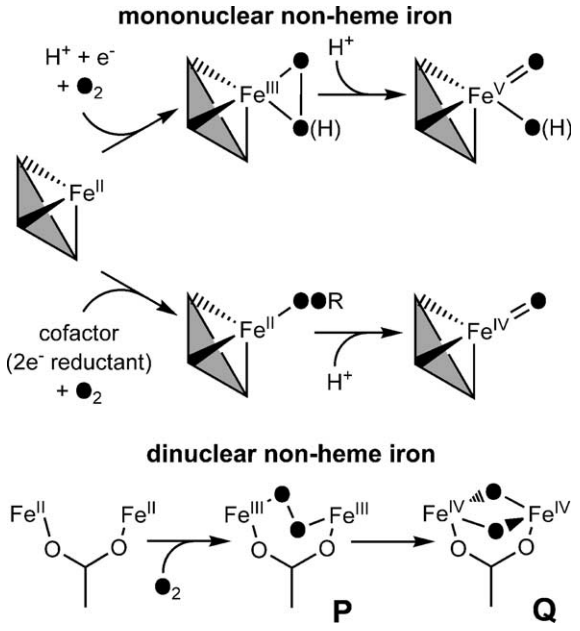

Scheme 1. General pathways for the activation of dioxygen to yield high-valent iron-oxo intermediates in both mononuclear and dinuclear non-heme iron enzymes.

binding to the diiron(II) center, forming a μ-1,2-peroxo diiron(III) complex, termed intermediate **P** (or H_{peroxo}) in the MMOH catalytic cycle. The O—O bond then is cleaved to yield an oxo-bridged diiron(IV) moiety termed **Q** [1,5]. Oxidative transformation of the substrate may be effected by either of these species [12]. Moreover, the situation can be further complicated by one-electron steps, which are required for the assembly of the diiron-tyrosyl radical center of the R2 protein of ribonucleotide reductase from *Escherichia coli* [13].

O_2 activation in the non-heme iron enzyme family is a well-regulated process, as the substrate is typically required to prime the active-site iron for the binding and reduction of oxygen to generate high-valent iron-oxo intermediates [1,14]. Nevertheless, this process occasionally appears to break down, with unexpected results. Under certain circumstances, O_2 (or its reduced counterparts) can be activated in the absence of substrate in the active site, in which case the high-valent intermediate produced must find an alternative reductive outlet, typically at the expense of further catalytic activity, in a process termed oxidative inactivation. One reductive pathway, which has attracted much recent attention, involves the oxidation of an aromatic amino acid located near the active site to yield a hydroxylated amino acid residue. In some instances, these hydroxylated amino acids remain coordinated to the iron center, generating brightly colored complexes that are amenable to analysis by a variety of techniques, as shown in Table 1. Herein, we describe the oxidative self-hydroxylation of several non-heme iron enzymes, as well as the spectroscopic evidence used to characterize these modified enzymes.

Ribonucleotide reductase

Chronologically, a mutant form of ribonucleotide reductase R2 (RNR R2, from *E. coli*) was the first example of a self-hydroxylation process recognized in non-heme iron enzymes and was thus subjected to a detailed structural and spectroscopic analysis. The oxygen activation

Table 1
UV/vis absorption maxima and spectroscopic methods used to characterize non-heme iron enzymes that self-hydroxylate an aromatic amino acid residue

Residue	Oxidative modification	Enzyme	λ_{max} (nm)	ε_{max} (M^{-1} cm^{-1})	Spectroscopic methods
Phe	*m*-OH-Phe	Y122F/E238A R2	515	Not reported	XRD
		W48F/D84E R2	550	1000–2100	XRD, rR
		TyrH-7,8-dihydrobiopterin[a]	—	—	XRD
	Phenoxy radical	Y122H R2	—	—	ENDOR
	Tyrosinate	HPPD	595	2600	rR
		Y325F PheH	—	—	ESI-MS
Tyr	DOPA	F208Y R2	720	2500	XRD, rR
		Y122F/F208Y R2	ca. 700	Not reported	—
		W48F/F208Y R2	675	Not reported	Mössbauer
		TauD-α-KG	550	700	rR
		TauD-succinate	720	380	rR
		PMI	680	2100	rR
		HppE	680	450	rR
Trp	Hydroxyindole	TfdA-α-KG	580	1000	rR
		AlkB-α-KG	590	960	ESI-MS
		Y325F PheH	—	—	ESI-MS

Abbreviations: α-KG, α-ketoglutarate; AlkB, alkylated DNA repair enzyme; DOPA, dihydroxyphenylalanine; ENDOR, electron nuclear double resonance; ESI-MS, electrospray ionization mass spectrometry; HPPD, 4-hydroxyphenylpyruvate dioxygenase; HppE, (*S*)-2-hydroxypropylphosphonic acid epoxidase; PheH, phenylalanine hydroxylase; PMI, phosphomannose isomerase; R2, the R2 subunit of ribonucleotide reductase; rR, resonance Raman; TauD, taurine/α-KG dioxygenase; TfdA, 2,4-dichlorophenoxyacetate/α-KG dioxygenase; TyrH, tyrosine hydroxylase; XRD, X-ray diffraction.

[a] The observed self-hydroxylation [54] is an artifact of the crystallography conditions and is not catalytically relevant [55].

mechanism for R2 deviates from that of MMOH by the injection of an electron following the formation of **P**, producing an iron(III)–iron(IV) intermediate termed **X** [15–17]; **X** is then responsible for the generation of a one-electron oxidized tyrosyl radical (Y122•) adjacent to the dinuclear metal center [18,19]. This center initiates the reduction of ribonucleotides by forming a substrate radical in the active site of the R1 subunit [20,21] via a long-range electron transfer pathway [22–24]. Extensive site-directed mutagenesis studies on RNR R2 have revealed a diverse range of post-translationally generated self-hydroxylation products (cf. Table 1) and shed light on the factors contributing to its favored one-electron oxidation pathway, rather than the two-electron process observed in other evolutionarily related enzymes such as MMOH and soluble fatty acid desaturases [1,5].

Mutation of F208, one of the residues comprising a hydrophobic pocket that houses the reaction site for O_2 [25] and stabilizes the Y122 radical [26], to tyrosine results in the generation of a blue chromophore ($\lambda_{max} = 720$ nm, $\varepsilon = 2500\ M^{-1}\ cm^{-1}$) both in vivo and in vitro (upon the addition of iron(II) and O_2 to apoR2). Resonance Raman vibrations associated with this chromophore are characteristic of an iron(III)–catecholate complex [27]. X-ray crystallography confirmed a catecholate moiety (derived from Y208) chelated to Fe_a of the diiron(III) core, as shown in Fig. 1A [28]. These seminal studies demonstrate that the active site of R2 can support a two-electron oxidation outcome in addition to the wild-type one-electron oxidation of Y122.

Subsequent crystallographic studies on apo and diferrous F208Y R2 suggested that Y208 is bound to the iron site throughout the catechol formation cycle [25]. Moreover, oxidation of Y208 in F208Y R2 in the presence of isotopically labeled O_2 and H_2O demonstrated that the inserted oxygen atom derives from solvent [29]. Intriguingly, a small amount of a short-lived tyrosyl radical was also generated during in vitro reconstitution of F208Y R2, while radical formation was abolished in the double mutant Y122F/F208Y [28]. The identification of this radical as Y122• on the basis of electron paramagnetic resonance (EPR) studies [26,30] led to the suggestion that the reaction pathway for F208Y R2 may partition between hydroxylating Y208 (major pathway) and generating the wild-type product Y122• (minor pathway) [26], and a later study gave insight into the origin and control of this partitioning process [31]. A key step in the wild-type reaction is the rapid injection of a single electron from an exogenous reductant, which is believed to commit the reaction to a one-electron oxidation outcome (Y122•) [32]. Since Y208 is hydroxylated in F208Y R2 in preference to the normal reaction, Y208 presumably competes with the electron injection step by acting as an endogenous reductant. However, Y122• formation is favored in the F208Y mutant in the presence of a high concentration of ascorbate, which favors one-electron injection but is dependent upon a hydrogen-bond network involving the near-surface residue W48 acting as an electron-transfer pathway into the diiron active site [22,33–35]. Significantly, the W48F/F208Y mutant inhibits the electron-transfer pathway, irrespective of the ascorbate concentration, thus strongly favoring Y208 hydroxylation. Therefore, the electron injection step (mediated by the electron-transfer pathway) may ensure that an intermediate containing two oxidizing equivalents is not generated during the normal reaction in R2, thereby precluding self-hydroxylation reactions that could compete with the one-electron oxidation of Y122.

Based on the premise that the introduction of non-native mutations such as F208Y in the active site may engender reactivity that is not relevant to the wild-type protein, another double mutant, W48F/D84E R2, was engineered to enforce a two-electron oxidation outcome while retaining a ligand set characteristic of the diiron-carboxylate family [36]. Exposure of W48F/D84E R2 to O_2 gives rise to a transient μ-1,2-peroxodiiron(III) species [37], which appears to be structurally similar to intermediate **P** in MMOH [38,39]. X-ray crystallographic analysis of the vividly purple-colored product ($\lambda_{max} = 550$ nm, $\varepsilon = 1000$–$2100\ M^{-1}\ cm^{-1}$) generated by decay of this **P**-like species revealed hydroxylation at the *meta* position of F208 [36]. Interestingly, resonance Raman spectroscopic studies of the purple chromophore demonstrated that the oxygen atom incorporated into F208 derives from O_2, rather than H_2O [36], in contrast to the solvent derived oxygen in F208Y R2 [29]. The contrasting labeling results observed for the F208Y and W48F/E238A self-hydroxylation reactions raise the possibility that subtly different oxidizing species are responsible for the transformation [36].

Two further instances of hydroxylation of F208 in mutant R2 enzymes have been reported. First, a crystal structure of the double mutant Y122F/E238A R2, in which one of the ligands of Fe_b (E238) was removed by mutation, also revealed hydroxylation of F208 at the *meta* position, with a relatively long 2.8 Å coordination to Fe_b, as indicated in Fig. 1B (λ_{max} ca. 475 and 515 nm) [25]. When combined with the crystallographic data for F208Y R2, this result suggests that the ligands of the diiron site contribute towards control of the reaction direction in R2. In particular, the hydroxylating species of F208Y R2 resembles the wild-type situation in which the high-valent species is exposed on Fe_a near Y122, resulting in the observed partitioning between Y208 hydroxylation and Y122• formation. Conversely, Y122F/E238A R2 presents a defective activation since the oxidizing species is exposed on the wrong iron atom as a result of the lower coordination number of Fe_b caused by the introduction of an alanine residue at position 238. Therefore, the iron ligand E238 appears to play a role in directing the reactivity of the activated oxygen species, thereby protecting R2 from harmful self-oxidation reactions [25].

In the second example, electron nuclear double resonance (ENDOR) studies on the R2 mutant Y122H, which was engineered in an attempt to generate a histidine radical at position 122, revealed that the enzyme contains a small

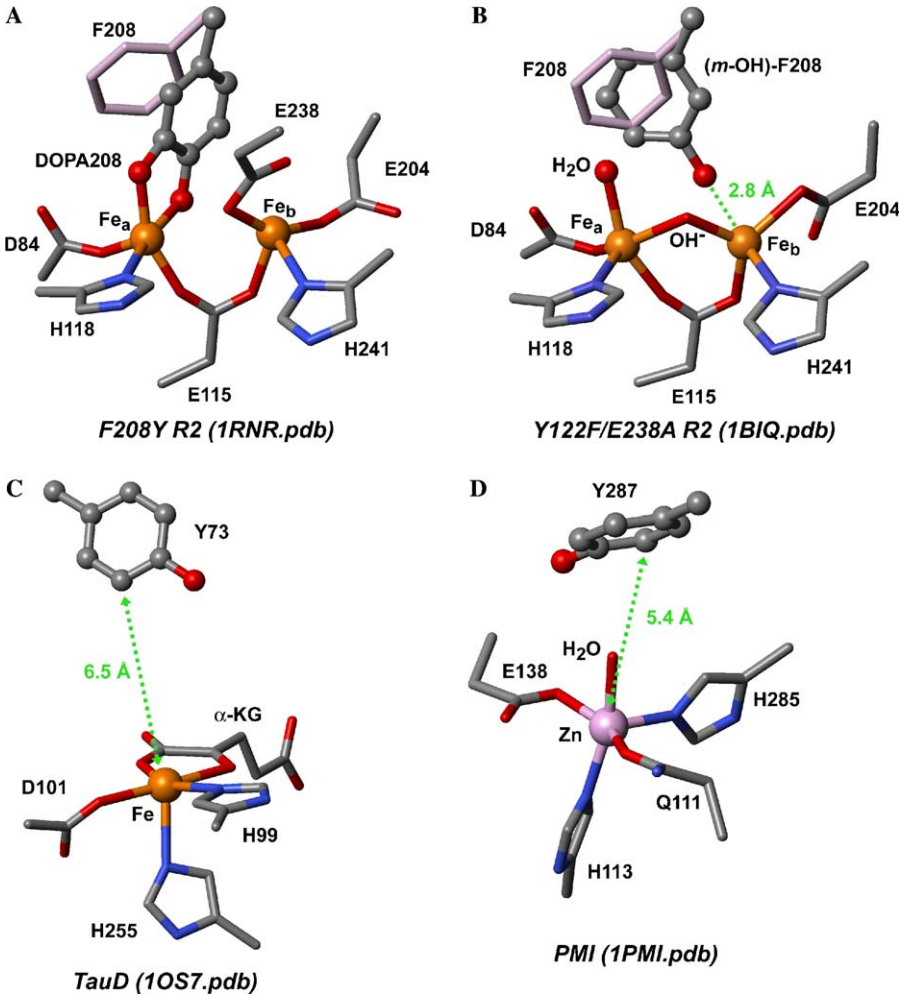

Fig. 1. Active site structures of crystallized non-heme iron enzymes showing either the self-hydroxylated residue or proximity of that residue to the metal center. (A) The Fe(III)–catecholate complex generated in F208Y R2 (1RNR.pdb). Shown in light pink is the position of F208 in the crystal structure of diferric wild-type R2 (1RIB.pdb). The image was generated by alignment of the two active sites using both Fe atoms, E115, H241, H118, and Y122 (not shown) as anchors. The oxo bridge in diferric wild-type R2 is not present in the oxidized F208Y crystal structure and is not shown for clarity. (B) The 2.8 Å interaction between Fe and *meta*-hydroxylated F208 in oxidized Y122F/E238A R2 (1BIQ.pdb). Hydroxylation was observed in only one subunit of the dimeric protein [25], and the position of non-hydroxylated F208 in the second subunit is shown in light pink. The image was generated by alignment of the active sites of the two subunits using the same anchor points as in (A). (C) The crystal structure of the active site of Fe(II)TauD with α-KG bound (taurine is not shown) shows the proximity of Y73 to the metal center prior to self-hydroxylation (1OS7.pdb). (D) The crystal structure of the Zn(II)PMI active site shows the position of Y257 relative to the metal center prior to self-hydroxylation (1PMI.pdb). Self-hydroxylation is not seen in the native Zn(II) protein but is observed upon Fe(II) substitution [58].

amount (ca. 5%) of a stable paramagnetic species, termed center **H**, that was proposed to be a diferric center with a strongly coupled radical [40]. Recently, a more detailed spectroscopic characterization of this mutant utilizing EPR and ENDOR spectroscopies with specific isotope labels on the ligands of the diferric cluster, as well as MALDI-TOF mass spectrometry of trypsin-digested Y122H and wild-type R2, suggested that center **H** is a diferric center strongly coupled to a phenoxy radical, with hydroxylation likely taking place at the *para* position of the ring, rather than the *meta* position [41]. Since F208 is the only Phe residue proximate to the iron site, this residue was proposed to be the likely target for hydroxylation, with subsequent one-electron oxidation yielding a phenoxy radical. The absence of evidence for a histidine radical suggests that either intermediate **X** is not powerful enough to generate a histidine radical, or else the oxidation of F208 to form a coordinating phenoxy radical is energetically more favorable [41]. Taken together, these three examples of self-hydroxylation at F208 in R2 are an especially impressive illustration of the oxidative power of the iron-oxo intermediate, which not only attacks the aromatic ring of tyrosine but also that of the more inert phenylalanine.

Mononuclear non-heme iron enzymes

Self-hydroxylation reactions have also been demonstrated for a number of members of a superfamily of mononuclear non-heme iron enzymes possessing a common active-site structure termed the 2-His-1-carboxylate

facial triad [14], a recurring motif which acts as a versatile platform for the activation of dioxygen. Included within this superfamily are the α-ketoglutarate (α-KG)-dependent dioxygenases, which catalyze a diverse range of metabolic transformations [3]. It has long been known that α-KG-dependent dioxygenases undergo uncoupled reactions and self-inactivate in the absence of prime substrate [1]. The earliest such examples involved the prolyl and lysyl hydroxylases, in which uncoupled turnover was shown to result in metal oxidation that was reversible by the addition of ascorbic acid [42]. More recently, the self-hydroxylation of a phenylalanine, tyrosine, or tryptophan residue has been reported (or suggested) for a number of different α-KG-dependent enzymes in the absence of substrate.

The α-KG-dependent enzyme taurine/α-KG dioxygenase (TauD) utilizes Fe(II), α-KG, and O_2 to hydroxylate taurine [43]. Recent work has shown a complex surface of pathways leading to the generation of a green chromophore in the uncoupled reaction of TauD with O_2 as well as insight into the identity of the hydroxylating intermediate. Exposure of the lilac-colored Fe(II)TauD–α-KG complex ($\lambda_{max} = 530$ nm, $\varepsilon_{530} = 140\ M^{-1}\ cm^{-1}$ [44]) to O_2 in the absence of taurine generates a transient yellow species ($\lambda_{max} = 408$ nm, $\varepsilon_{408} \geqslant 1600\ M^{-1}\ cm^{-1}$) en route to the formation of a greenish-brown chromophore ($\lambda_{max} = 550$ nm, $\varepsilon_{550} = 700\ M^{-1}\ cm^{-1}$) [45]. The latter displays resonance Raman vibrations consistent with the formation of an Fe(III)–catecholate moiety arising from the self-hydroxylation of an active site tyrosine residue [45]. This residue has been identified by site-directed mutagenesis as Y73, which is ca. 6.5 Å away from the Fe center (Fig. 1C).

The hydroxylation of Y73 in TauD demonstrates that the Fe(II)TauD–α-KG complex can activate O_2 even in the absence of substrate, albeit more slowly. The active oxidant oxidizes Y73 first to a tyrosyl radical, corresponding to the yellow intermediate (as shown by EPR analysis [45]), which is subsequently converted to a catecholate. Interestingly, isotope-labeling resonance Raman studies show that the incorporated oxygen derives from solvent [45]. These spectroscopic results implicate an oxidant that can exchange with solvent, most likely the oxoiron(IV) species recently identified in transient kinetic studies of the reaction of the ternary Fe(II)TauD–α-KG–taurine complex with O_2 [8,11,46,47].

A second bright green chromophore ($\lambda_{max} = 720$ nm, ε_{720} ca. $300\ M^{-1}\ cm^{-1}$) arises from the O_2-dependent self-hydroxylation of Fe(II)TauD in the presence of succinate, the decarboxylated product of α-KG [48]. Resonance Raman spectroscopy reveals that the succinate-derived 720 nm chromophore also arises from an iron(III)–catecholate complex [48]. The species responsible for this bright green chromophore is related to that of the α-KG-derived brownish green chromophore by a bicarbonate binding equilibrium. For example, upon the addition of excess bicarbonate the 720 nm species slowly converts to the 550 nm chromophore [48]. Conversely, the 550 nm chromophore converts to the 720 nm species upon standing for several days (or incubation with taurine for two hours). The color changes reflect a modulation of the Lewis acidity of the metal center by the interchange between anionic bicarbonate and a neutral solvent ligand.

While the self-hydroxylation reaction of TauD has been investigated in considerable detail, there are other examples of similar reactions amongst the α-KG-dependent dioxygenases. In the case of the herbicide degrading 2,4-dichlorophenoxyacetate/α-KG dioxygenase (TfdA), exposure of the Fe(II)TfdA–α-KG complex to O_2 results in the formation of a blue chromophore (λ_{max} ca. 580 nm, ε ca. $1000\ M^{-1}\ cm^{-1}$) [49]. Resonance Raman experiments reveal ligand vibrations distinct from those of a phenolate or a catecholate but similar to those of 5-hydroxyindole, implying the hydroxylation of a tryptophan residue [49]. This residue has been identified as W112 on the basis of electrospray mass spectral analysis. Furthermore, labeling experiments show that the incorporated oxygen atom derives from solvent [49], as with TauD, suggesting that a common self-hydroxylation mechanism is operative in the α-KG-dependent dioxygenases. A blue chromophore ($\lambda_{max} = 590$ nm, $\varepsilon = 960\ M^{-1}\ cm^{-1}$) is also generated under similar conditions in the case of AlkB, an α-KG-dependent enzyme that repairs methylated bases in DNA and RNA [50]. The hydroxylated residue has been identified by ESI-MS to be W178. Notably, this self-hydroxylation was also observed in a control sample, implying that W178 may be hydroxylated in vivo [50].

Self-hydroxylation of a phenylalanine residue may occur in the case of 4-hydroxyphenylpyruvate dioxygenase (HPPD), an α-ketoacid-dependent enzyme involved in tyrosine catabolism. The isolated, oxidized enzyme exhibits a blue color (λ_{max} ca. 595 nm, $\varepsilon = 2600\ M^{-1}\ cm^{-1}$ [51]) that arises from a tyrosinate-to-iron(III) LMCT transition, as demonstrated by resonance Raman spectroscopy [52]. However, the subsequent crystal structure of the reduced enzyme [53] shows the iron(II) center coordinated to a characteristic 2-His-1-carboxylate facial triad motif with no coordinated tyrosine ligand. This result suggests that the chromophore may result from the uncoupled self-hydroxylation of a nearby phenylalanine residue.

Self-hydroxylation reactions also occur in several pterin-dependent hydroxylases. Crystallographic studies of tyrosine hydroxylase (TyrH) show the active site residue F300 to be hydroxylated in two structures, one of the catalytic domains crystallized in the presence of the substrate analog 7,8-dihydrobiopterin and the other of the catalytic and tetramerization domains [54]. Subsequently, MALDI-TOF mass spectrometry and amino acid sequencing demonstrated that F300 is only hydroxylated in the isolated catalytic domain upon incubation with an excess of 7,8-dihydrobiopterin, the reductant DTT, and Fe(II) in the absence of substrate [55], indicating that the observed hydroxylation was likely an artifact of the crystallography conditions. More recently, studies have shown that the Y325F mutant of human phenylalanine hydroxylase (PheH) has an activ-

ity identical to that of the wild-type enzyme [56,57]. ESI-MS analyses of trypsin digests of the Y325F variant and wild-type PheH revealed the in vivo hydroxylation of F325 in Y325F PheH to tyrosine, as well as possible hydroxylation of an outer-sphere tryptophan residue [57]. Y325 is thought to be involved in hydrogen bonding interactions that stabilize binding of the pterin cofactor; thus, this example may represent an instance of enzyme self-repair.

Self-hydroxylation processes have also been described for two other mononuclear non-heme enzymes with a 2-His-1-carboxylate metal binding site. In the first instance, the substitution of iron for the native zinc ion in recombinant phosphomannose isomerase (PMI) leads to the development of a green chromophore ($\lambda_{max} = 680$ nm, $\varepsilon = 2100\ M^{-1}\ cm^{-1}$/Fe) attributable to hydroxylation of Y257 (as demonstrated by resonance Raman spectroscopy [58]), which is ca. 5.4 Å distant from the metal center in the Zn(II) crystal structure (Fig. 1D) [59]. Likewise, (*S*)-hydroxypropylphosphonic acid epoxidase (HppE), which catalyzes the formation of the antibiotic fosfomycin [60], also develops a green color ($\lambda_{max} = 680$ nm, $\varepsilon = 450\ M^{-1}\ cm^{-1}$) as a result of tyrosine self-hydroxylation (likely Y105) upon reconstitution of the apo enzyme with Fe(II) under aerobic conditions [61]. Isotope-labeling resonance Raman experiments demonstrated that oxygen is not incorporated into the catechol from either O_2 or H_2O, indicating that the post-translational modification event occurs in vivo [61]. Reconstitution of the enzyme under O_2 in the presence of excess ascorbate generated a greater yield of the green chromophore, with the incorporated oxygen deriving from O_2, as demonstrated by isotope-labeling studies [61]. This observation implies that ascorbate provides the electrons necessary to activate dioxygen, a role similar to that of pterin and α-KG in pterin- and α-KG-dependent dioxygenases, respectively [61].

Mechanistic implications

The self-hydroxylation reactions described above serve as probes for the mechanisms of oxygen activation at non-heme iron sites, as these transformations give rise to visible chromophores readily probed by resonance Raman spectroscopy to reveal the source of the oxygen atom (either from O_2 or water) that is incorporated into the residue. Although high-valent iron-oxo species are generally believed to be involved in biological oxidations catalyzed by iron centers, there has been recent discussion regarding the possibility that metal-peroxo species may also be involved under some circumstances [7,12,62]. For self-hydroxylation reactions, the fact that solvent-derived oxygen can be incorporated in several examples excludes the possibility of a direct oxygen-atom transfer from a metal-peroxo species and requires O—O bond cleavage to occur prior to C—O bond formation in order to allow the active oxygen species to exchange with solvent water.

An oxoiron(IV) intermediate has been demonstrated to serve as the kinetically competent oxidant in the wild-type TauD reaction [8,11,46,47]. This species is proposed to form via a mechanism first proposed in 1982 by Hanauske-Abel (Scheme 2) for the α-KG-dependent dioxygenases [63]. This mechanism involves the initial binding of O_2 to the binary Fe(II)enzyme–α-KG complex, generating an iron(III)-superoxo species. Nucleophilic attack by the

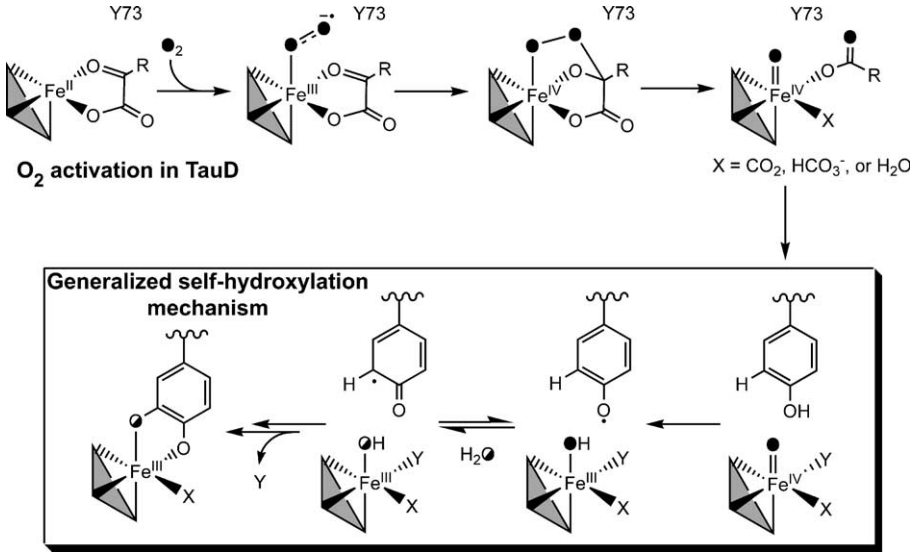

Scheme 2. Proposed mechanism for the self-hydroxylation of a nearby tyrosine residue in mononuclear non-heme iron enzymes utilizing an oxoiron(IV) intermediate as the oxidant. The three protein-derived ligands which form the 2-His-1-carboxylate facial triad are shown as a shaded triangle. Shown first is the specific pathway for O_2 activation in the α-KG-dependent dioxygenases. It should be noted that following the decarboxylation of α-KG, there are several possibilities for the identity of the ligand at position X, including CO_2, HCO_3^-, H_2O, or an equilibrium mixture thereof. The boxed portion depicts a more general process for hydroxylation of a tyrosine residue through a tyrosyl radical, where ligands X and Y are variable. O_2-derived oxygen atoms are depicted as filled circles, with half-filled circles reflecting the possibility of exchange with H_2O.

terminal superoxo oxygen onto the α-keto carbon of α-KG affords a yet unobserved peroxo species that undergoes subsequent C—C and O—O bond cleavage to generate the oxoiron(IV) intermediate with CO_2 and succinate as by-products. The fact that self-hydroxylation occurs in TauD shows that oxygen activation can occur even in the absence of substrate, albeit more slowly. Instead of oxidizing taurine, the Fe(IV)=O species hydroxylates the nearby Y73 residue.

The resonance Raman experiments on self-hydroxylated TauD establish that the incorporated oxygen atom derives from water. Thus, solvent exchange with the oxidizing species in TauD must occur prior to the formation of the C—O bond. Although the nature of the taurine hydroxylation product does not allow the source of its oxygen atom to be established by product analysis, it is clear from the resonance Raman data on the Fe(IV)=O intermediate derived from the enzyme–cofactor–substrate complex that solvent exchange does not occur within the lifetime of that intermediate [9]. To rationalize the labeling result for the self-hydroxylated TauD, it is necessary to postulate that either the presence of substrate serves to restrict access of solvent water into the active site, thereby hindering oxygen atom exchange with the Fe(IV)=O species observed in taurine hydroxylation, or that the exchange occurs at a subsequent stage of the self-hydroxylation reaction but prior to C—O bond formation. A tyrosyl radical intermediate has been identified as the precursor to the catecholate chromophore in TauD [45]. This observation indicates that the first step of Y73 oxidation involves the abstraction of its O—H hydrogen atom by the Fe(IV)=O intermediate to form the tyrosyl radical and an Fe(III)—OH center (Scheme 2). Solvent exchange with the latter prior to oxygen rebound with the aromatic radical introduces label from $H_2{}^{18}O$ into the catecholate ring. Similar solvent label incorporation into the hydroxylated tryptophan residue of TfdA suggests a comparable mechanism is likely to be operative in this reaction as well [49].

The newly introduced oxygen atom in DOPA208 R2 similarly derives from water, suggesting that the diiron center of R2 can perform chemistry analogous to the mononiron centers of TauD and TfdA. Again, O—O bond cleavage must precede C—O bond formation to account for water-derived oxygen incorporation into the DOPA residue. Oxygen activation by the diiron site of R2 is proposed to follow a mechanism analogous to that proposed for MMOH involving initial formation of a peroxodiiron(III) intermediate (**P** in Scheme 1), as demonstrated for the D84E and W48F/D84E R2 mutants [36–39]. In wild-type R2, injection of an electron from an exogenous reductant converts this **P**-like species into the iron(III)–iron(IV) intermediate **X** [15–17], which is the oxidant of Y122. For F208Y R2, however, the nearby Y208**.** residue [25] can instead provide an electron that effects cleavage of the O—O bond. This electron transfer step presumably leads to a putative Y208•/iron(III)–iron(IV) species that must have a sufficient lifetime to permit solvent exchange before subsequently collapsing to the diiron(III)–catecholate chromophore (Scheme 3).

In contrast, the oxygen atom incorporated into F208 in the self-hydroxylation of W48F/D84E R2 derives from O_2 [36]. Unlike for F208Y R2, intermediate **X** does not accumulate in the reaction sequence for W48F/D84E R2, suggesting that this intermediate either does not participate

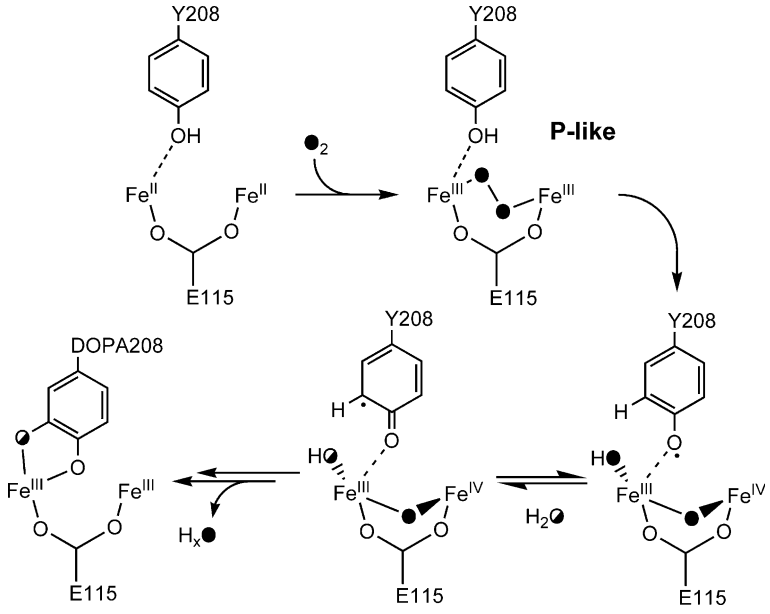

Scheme 3. Proposed mechanism for the self-hydroxylation of Y208 in F208Y R2 to afford an Fe(III)–catecholate product, consistent with the crystallographic observation of a weak interaction between Fe and Y208 in the initial diferrous state. The μ-1,2-peroxodiiron(III) species analogous to intermediate **P** of MMOH is labeled as such. For clarity, ligands other than the bridging residue E115 are not shown. O_2-derived oxygen atoms are shown as filled circles, with the half-filled circles reflecting the possibility of exchange with H_2O. The second bridging oxygen derived from O_2 is thought to depart as either hydroxide or water [29,36].

in the hydroxylation mechanism in this mutant or has too short a lifetime to allow solvent exchange [36]. The analogous one-electron transfer from F208 to the **P**-like intermediate would be expected to have a higher activation barrier, since a phenylalanine residue is not a very good one-electron reductant. Alternatively, direct oxygen-atom transfer from the **P**-like intermediate to F208 would account for the observed oxygen-atom incorporation from O_2. Such an oxygen-atom transfer has also been recently observed in MMOH, in which intermediate **P** is shown to effect the epoxidation of olefins [64], a result that may well reflect the mechanistic diversity of non-heme iron enzymes.

The in vitro self-hydroxylation of HppE also results in oxygen incorporation from O_2, in contrast to TauD and other α-KG-dependent dioxygenases, with ascorbate required as an exogenous reductant [61]. Assuming that ascorbate acts as a one-electron reductant, the incorporation of oxygen from O_2 suggests that oxygen activation proceeds via an Fe(III)–OOH intermediate (Scheme 1), as implicated for the Rieske dioxygenases [2]. This intermediate may hydroxylate the nearby tyrosine residue directly or convert to an HO–Fe(V)═O oxidant that does not undergo solvent exchange prior to attacking tyrosine. Additional mechanistic and spectroscopic analyses should give further insight into this intriguing transformation.

In closing, Nature employs a variety of redox centers to carry out oxygenation reactions, often utilizing iron centers to generate powerful oxidizing species that carry out energetically difficult transformations. Occasionally, uncoupling can result in self-hydroxylation of nearby aromatic amino acids by these high-valent iron-oxo species, as observed for a number of non-heme iron enzymes. In some cases, this process may serve to protect enzyme active sites from the inimical effects of adventitious oxygen activation in the absence of substrate [49,65] or may even provide a mechanism for enzyme repair [57]; in others, they may simply be aberrations that serve no physiological function. Nevertheless, the several well-studied examples of self-hydroxylation processes have shed light into the mechanisms of oxygen activation at non-heme iron centers and have contributed towards our understanding of the delicate dance between iron and O_2 in achieving a remarkable range of oxidative transformations.

References

[1] E.I. Solomon, T.C. Brunold, M.I. Davis, J.N. Kemsley, S.-K. Lee, N. Lehnert, F. Neese, A.J. Skulan, Y.-S. Yang, J. Zhou, Geometric and electronic structure/function correlations in non-heme iron enzymes, Chem. Rev. 100 (2000) 235–349.

[2] M. Costas, M.P. Mehn, M.P. Jensen, L. Que Jr., Dioxygen activation at mononuclear nonheme iron active sites: enzymes, models, and intermediates, Chem. Rev. 104 (2004) 939–986.

[3] R.P. Hausinger, Fe(II)/α-ketoglutarate-dependent hydroxylases and related enzymes, Crit. Rev. Biochem. Mol. Biol. 39 (2004) 21–68.

[4] B.J. Wallar, J.D. Lipscomb, Dioxygen activation by enzymes containing binuclear non-heme iron clusters, Chem. Rev. 96 (1996) 2625–2657.

[5] M. Merkx, D.A. Kopp, M.H. Sazinsky, J.L. Blazyk, J. Müller, S.J. Lippard, Dioxygen activation and methane hydroxylation by soluble methane monooxygenase: a tale of two irons and three proteins, Angew. Chem. Int. Ed. 40 (2001) 2782–2807.

[6] M. Sono, M.P. Roach, E.D. Coulter, J.H. Dawson, Heme-containing oxygenases, Chem. Rev. 96 (1996) 2841–2887.

[7] S. Jin, T.A. Bryson, J.H. Dawson, Hydroperoxoferric heme intermediate as a second electrophilic oxidant in cytochrome P450-catalyzed reactions, J. Biol. Inorg. Chem. 9 (2004) 644–653.

[8] J.C. Price, E.W. Barr, B. Tirupati, J.M. Bollinger Jr., C. Krebs, The first direct characterization of a high-valent iron intermediate in the reaction of an α-ketoglutarate-dependent dioxygenase: a high-spin Fe(IV) complex in taurine/α-ketoglutarate dioxygenase (TauD) from *Escherichia coli*, Biochemistry 42 (2003) 7497–7508.

[9] D.A. Proshlyakov, T.F. Henshaw, G.R. Monterosso, M.J. Ryle, R.P. Hausinger, Direct detection of oxygen intermediates in the non-heme Fe enzyme taurine/α-ketoglutarate dioxygenase, J. Am. Chem. Soc. 126 (2004) 1022–1023.

[10] P.J. Riggs-Gelasco, J.C. Price, R.B. Guyer, J.H. Brehm, E.W. Barr, J.M. Bollinger Jr., C. Krebs, EXAFS spectroscopic evidence for an Fe═O unit in the Fe(IV) intermediate observed during oxygen activation by taurine:α-ketoglutarate dioxygenase, J. Am. Chem. Soc. 126 (2004) 8108–8109.

[11] J.C. Price, E.W. Barr, T.E. Glass, C. Krebs, J.M. Bollinger Jr., Evidence for hydrogen abstraction from C1 of taurine by the high-spin Fe(IV) intermediate detected during oxygen activation by taurine:α-ketoglutarate dioxygenase (TauD), J. Am. Chem. Soc. 125 (2003) 13008–13009.

[12] L. Que Jr., The oxo/peroxo debate: a nonheme iron perspective, J. Biol. Inorg. Chem. 9 (2004) 684–690.

[13] J. Stubbe, P. Riggs-Gelasco, Harnessing free radicals: formation and function of the tyrosyl radical in ribonucleotide reductase, Trends Biol. Sci. 23 (1998) 438–443.

[14] K.D. Koehntop, J.P. Emerson, L. Que Jr., The 2-His-1-carboxylate facial triad: a versatile platform for dioxygen activation by mononuclear nonheme iron(II) enzymes, J. Biol. Inorg. Chem. 10 (2005) 87–93.

[15] B.E. Sturgeon, D. Burdi, S. Chen, B.-H. Huynh, D.E. Edmondson, J. Stubbe, B.M. Hoffman, Reconsideration of X, the diiron intermediate formed during cofactor assembly in *E. coli* ribonucleotide reductase, J. Am. Chem. Soc. 118 (1996) 7551–7557.

[16] J.-P. Willems, H.-I. Lee, D. Burdi, P.E. Doan, J. Stubbe, B.M. Hoffman, Identification of the protonated oxygenic ligands of ribonucleotide reductase intermediate X by Q-band ^{1,2}H CW and pulsed ENDOR, J. Am. Chem. Soc. 119 (1997) 9816–9824.

[17] P.J. Riggs-Gelasco, L. Shu, S. Chen, D. Burdi, B.H. Huynh, L. Que Jr., J. Stubbe, EXAFS characterization of the intermediate **X** generated during the assembly of the *Escherichia coli* ribonucleotide reductase R2 diferric tyrosyl radical cofactor, J. Am. Chem. Soc. 120 (1998) 849–860.

[18] B.-M. Sjöberg, P. Reichard, A. Gräslund, A. Ehrenberg, Nature of the free radical in ribonucleotide reductase from *Escherichia coli*, J. Biol. Chem. 252 (1977) 536–541.

[19] A. Larsson, B.-M. Sjöberg, Identification of the stable free radical tyrosine residue in ribonucleotide reductase, EMBO J. 5 (1986) 2037–2040.

[20] J. Stubbe, D. Ackles, On the mechanism of ribonucleoside diphosphate reductase from *Escherichia coli*. Evidence for 3′-C─H bond cleavage, J. Biol. Chem. 255 (1980) 8027–8030.

[21] B.-M. Sjöberg, A. Gräslund, F. Eckstein, A substrate radical intermediate in the reaction between ribonucleotide reductase from *Escherichia coli* and 2′-azido-2′-deoxynucleoside diphosphates, J. Biol. Chem. 258 (1983) 8060–8067.

[22] P. Nordlund, H. Eklund, Structure and function of the *Escherichia coli* ribonucleotide reductase protein R2, J. Mol. Biol. 232 (1993) 123–164.

[23] U. Uhlin, H. Eklund, Structure of ribonucleotide reductase protein R1, Nature 370 (1994) 533–539.

[24] B.-M. Sjöberg, The ribonucleotide reductase jigsaw puzzle: a large piece falls into place, Structure 2 (1994) 793–796.
[25] D.T. Logan, F. deMaré, B.O. Persson, A. Slaby, B.-M. Sjöberg, P. Nordlund, Crystal structures of two self-hydroxylating ribonucleotide reductase protein R2 mutants: structural basis for the oxygen-insertion step of hydroxylation reactions catalyzed by diiron proteins, Biochemistry 37 (1998) 10798–10807.
[26] M. Ormö, K. Regnström, Z. Wang, L. Que Jr., M. Sahlin, B.-M. Sjöberg, Residues important for radical stability in ribonucleotide reductase from *Escherichia coli*, J. Biol. Chem. 270 (1995) 6570–6576.
[27] M. Ormö, F. deMaré, K. Regnström, A. Åberg, M. Sahlin, J. Ling, T.M. Loehr, J. Sanders-Loehr, B.-M. Sjöberg, Engineering of the iron site in ribonucleotide reductase to a self-hydroxylating monooxygenase, J. Biol. Chem. 267 (1992) 8711–8714.
[28] A. Åberg, M. Ormö, P. Nordlund, B.-M. Sjöberg, Autocatalytic generation of dopa in the engineered protein R2 F208Y from *Escherichia coli* ribonucleotide reductase and crystal structure of the dopa-208 protein, Biochemistry 32 (1993) 9845–9850.
[29] J. Ling, M. Sahlin, B.-M. Sjöberg, T.M. Loehr, J. Sanders-Loehr, Dioxygen is the source of the μ-oxo bridge in iron ribonucleotide reductase, J. Biol. Chem. 269 (1994) 5595–5601.
[30] A. Liu, M. Sahlin, S. Pötsch, B.-M. Sjöberg, A. Gräslund, New paramagnetic species formed at the expense of the transient tyrosyl radical in mutant protein R2 F208Y of *Escherichia coli* ribonucleotide reductase, Biochem. Biophys. Rec. Commun. 246 (1998) 740–745.
[31] S.E. Parkin, S. Chen, B.A. Ley, L. Mangravite, D.E. Edmondson, B.H. Huynh, J.M. Bollinger Jr., Electron injection through a specific pathway determines the outcome of oxygen activation at the diiron cluster in the F208Y mutant of *Escherichia coli* ribonucleotide reductase protein R2, Biochemistry 37 (1998) 1124–1130.
[32] W.H. Tong, S. Chen, S.G. Lloyd, D.E. Edmonson, B.H. Huynh, J. Stubbe, Mechanism of assembly of the diferric cluster-tyrosyl radical cofactor of *Escherichia coli* ribonucleotide reductase from the diferrous form of the R2 subunit, J. Am. Chem. Soc. 118 (1996) 2107–2108.
[33] J.M. Bollinger Jr., W.H. Tong, N. Ravi, B.H. Huynh, D.E. Edmondson, J. Stubbe, Mechanism of assembly of the tyrosyl radical-diiron(III) cofactor of *E. coli* ribonucleotide reductase. 3. Kinetics of the limiting Fe^{2+} reaction by optical, EPR, and Mössbauer spectroscopies, J. Am. Chem. Soc. 116 (1994) 8024–8032.
[34] U. Rova, K. Goodtzova, R. Ingemarson, G. Behravan, A. Gräslund, L. Thelander, Evidence by site-directed mutagenesis supports long-range electron transfer in mouse ribonucleotide reductase, Biochemistry 34 (1995) 4267–4275.
[35] M. Ekberg, M. Sahlin, M. Eriksson, B.-M. Sjöberg, Two conserved tyrosine residues in protein R1 participate in an intermolecular electron transfer in ribonucleotide reductase, J. Biol. Chem. 271 (1996) 20655–20659.
[36] J. Baldwin, W.C. Voegtli, N. Khidekel, P. Moënne-Loccoz, C. Krebs, A.S. Pereira, B.A. Ley, B.H. Huynh, T.M. Loehr, P.J. Riggs-Gelasco, A.C. Rosenzweig, J.M. Bollinger Jr., Rational reprogamming of the R2 subunit of *Escherichia coli* ribonucleotide reductase into a self-hydroxylating monooxygenase, J. Am. Chem. Soc. 123 (2001) 7017–7030.
[37] J. Baldwin, C. Krebs, L. Saleh, M. Stelling, B.H. Huynh, J.M. Bollinger Jr., P. Riggs-Gelasco, Structural characterization of the peroxodiiron(III) intermediate generated during oxygen activation by the W48A/D84E variant of ribonucleotide reductase protein R2 from *Escherichia coli*, Biochemistry 42 (2003) 13269–13279.
[38] J.M. Bollinger Jr., C. Krebs, A. Vicol, S. Chen, B.A. Ley, D.E. Edmondson, B.H. Huynh, Engineering the diiron site of *Escherichia coli* ribonucleotide reductase protein R2 to accumulate an intermediate similar to H_{peroxo}, the putative peroxodiiron(III) complex from the methane monooxygenase catalytic cycle, J. Am. Chem. Soc. 120 (1998) 1094–1095.
[39] P. Moënne-Loccoz, J. Baldwin, B.A. Ley, T.M. Loehr, J.M. Bollinger Jr., O_2 activation by non-heme diiron proteins: identification of a symmetric μ-1,2-peroxide in a mutant of ribonucleotide reductase, Biochemistry 37 (1998) 14659–14663.
[40] M. Kolberg, G. Bleifuss, S. Pötsch, A. Gräslund, W. Lubitz, G. Lassmann, F. Lendzian, A new stable high-valent diiron center in R2 mutant Y122H of *E. coli* ribonucleotide reductase studied by high-field EPR and ^{57}Fe-ENDOR, J. Am. Chem. Soc. 122 (2000) 9856–9857.
[41] M. Kolberg, D.T. Logan, G. Bleifuss, S. Pötsch, B.-M. Sjöberg, A. Gräslund, W. Lubitz, G. Lassmann, F. Lendzian, A new tyrosyl radical on Phe^{208} as ligand to the diiron center in *Escherichia coli* ribonucleotide reductase, mutant R2-Y122H, J. Biol. Chem. 280 (2005) 11233–11246.
[42] R. Myllylä, K. Majamaa, V. Günzler, H.N. Hanauske-Abel, K.I. Kivirikko, Ascorbate is consumed stoichiometrically in the uncoupled reactions catalyzed by prolyl 4-hydroxylase and lysyl hydroxylase, J. Biol. Chem. 259 (1984) 5403–5405.
[43] E. Eichhorn, J.R. van der Ploeg, M.A. Kertesz, T. Leisinger, Characterization of α-ketoglutarate-dependent taurine dioxygenase from *Escherichia coli*, J. Biol. Chem. 272 (1997) 23031–23036.
[44] R.Y.N. Ho, M.P. Mehn, E.L. Hegg, A. Liu, M.J. Ryle, R.P. Hausinger, L. Que Jr., Resonance Raman studies of the iron(II)-α-keto acid chromophore in model and enzyme complexes, J. Am. Chem. Soc. 123 (2001) 5022–5029.
[45] M.J. Ryle, A. Liu, R.B. Muthukumaran, R.Y.N. Ho, K.D. Koehntop, J. McCracken, L. Que Jr., R.P. Hausinger, O_2- and α-ketoglutarate-dependent tyrosyl radical formation in TauD, an α-keto acid-dependent non-heme iron dioxygenase, Biochemistry 42 (2003) 1854–1862.
[46] J.C. Price, E.W. Barr, L.M. Hoffart, C. Krebs, J.M. Bollinger Jr., Kinetic dissection of the catalytic mechanism of taurine:α-ketoglutarate dioxygenase (TauD) from *Escherichia coli*, Biochemistry 44 (2005) 8138–8147.
[47] P.K. Grzyska, M.J. Ryle, G.R. Monterosso, J. Liu, D.P. Ballou, R.P. Hausinger, Steady-state and transient kinetic analyses of taurine/α-ketoglutarate dioxygenase: effects of oxygen concentration, alternative sulfonates, and active-site variants on the Fe^{IV}-oxo intermediate, Biochemistry 44 (2005) 3845–3855.
[48] M.J. Ryle, K.D. Koehntop, A. Liu, L. Que Jr., R.P. Hausinger, Interconversion of two oxidized forms of taurine/α-ketoglutarate dioxygenase, a non-heme iron hydroxylase: evidence for bicarbonate binding, Proc. Natl. Acad. Sci. USA 100 (2003) 3790–3795.
[49] A. Liu, R.Y.N. Ho, L. Que Jr., M.J. Ryle, B.S. Phinney, R.P. Hausinger, Alternative reactivity of an α-ketoglutarate-dependent iron(II) oxygenase: enzyme self-hydroxylation, J. Am. Chem. Soc. 123 (2001) 5126–5127.
[50] T.F. Henshaw, M. Feig, R.P. Hausinger, Aberrant activity of the DNA repair enzyme AlkB, J. Inorg. Biochem. 98 (2004) 856–861.
[51] S. Lindstedt, M. Rundgren, Blue color, metal content, and substrate binding in 4-hydroxyphenylpyruvate dioxygenase from *Pseudomonas sp.* Strain P.J. 874, J. Biol. Chem. 257 (1982) 11922–11931.
[52] F.C. Bradley, S. Lindstedt, J.D. Lipscomb, L. Que Jr., A.L. Roe, M. Rundgren, 4-Hydroxyphenylpyruvate dioxygenase is an iron-tyrosinate protein, J. Biol. Chem. 261 (1986) 11693–11696.
[53] L. Serre, A. Sailland, D. Sy, P. Boudec, A. Rolland, E. Pebay-Peyroula, C. Cohen-Addad, Crystal structure of *Pseudomonas fluorescens* 4-hydroxyphenylpyruvate dioxygenase: an enzyme involved in the tyrosine degradation pathway, Structure 7 (1999) 977–988.
[54] K.E. Goodwill, C. Sabatier, R.C. Stevens, Crystal structure of tyrosine hydroxylase with bound cofactor analogue and iron at 2.3 Å resolution: self-hydroxylation of Phe300 and the pterin-binding site, Biochemistry 37 (1998) 13437–13445.
[55] H.R. Ellis, S.C. Daubner, R.I. McCulloch, P.F. Fitzpatrick, Phenylalanine residues in the active site of tyrosine hydroxylase: mutagenesis of Phe300 and Phe309 to alanine and metal ion-catalyzed hydroxylation of Phe 300, Biochemistry 38 (1999) 10909–10914.
[56] H. Erlandsen, E. Bjørgo, T. Flatmark, R.C. Stevens, Crystal structure and site-specific mutagenesis of pterin-bound human phenylalanine hydroxylase, Biochemistry 39 (2000) 2208–2217.

[57] S.D. Kinzie, M. Thevis, K. Ngo, J. Whitelegge, J.A. Loo, M.M. Abu-Omar, Posttranslational hydroxylation of human phenylalanine hydroxylase is a novel example of enzyme self-repair within the second coordination sphere of catalytic iron, J. Am. Chem. Soc. 125 (2003) 4710–4711.
[58] J.J. Smith, A.J. Thomson, A.E. Proudfoot, T.N. Wells, Identification of an Fe(III)-dihydroxyphenylalanine site in recombinant phosphomannose isomerase from *Candida albicans*, Eur. J. Biochem. 244 (1997) 325–333.
[59] A. Cleasby, A. Wonacott, T. Skarzynski, R.E. Hubbard, G.J. Davies, A.E.I. Proudfoot, A.R. Bernard, M.A. Payton, T.N.C. Wells, The X-ray crystal structure of phosphomannose isomerase from *Candida albicans* at 1.7 Å resolution, Nat. Struct. Biol. 3 (1996) 470–479.
[60] L.J. Higgins, F. Yan, P. Liu, H.-W. Liu, C.L. Drennan, Structural insight into antibiotic fosfomycin biosynthesis by a mononuclear iron enzyme, Nature (2005), doi:10.1038/nature03924.
[61] P. Liu, M.P. Mehn, F. Yan, Z. Zhao, L. Que Jr., H.-W. Liu, Oxygenase activity in the self-hydroxylation of (*S*)-2-hydroxypropylphosphonic acid epoxidase involved in fosfomycin biosynthesis, J. Am. Chem. Soc. 126 (2004) 10306–10312.
[62] S. Shaik, S.P. de Visser, D. Kumar, One oxidant, many pathways: a theoretical perspective of monooxygenation mechanisms by cytochrome P450 enzymes, J. Biol. Inorg. Chem. 9 (2004) 661–668.
[63] H.M. Hanauske-Abel, V. Günzler, A stereochemical concept for the catalytic mechanism of prolyl hydroxylase. Applicability to classification and design of inhibitors, J. Theor. Biol. 94 (1982) 421–455.
[64] L.G. Beauvais, S.J. Lippard, Reactions of the peroxo intermediate of soluble methane monooxygenase hydroxylase with ethers, J. Am. Chem. Soc. 127 (2005) 7370–7378.
[65] J.N. Barlow, Z. Zhang, P. John, J.E. Baldwin, C.J. Schofield, Inactivation of 1-aminocyclopropane-1-carboxylate oxidase involves oxidative modifications, Biochemistry 36 (1997) 3563–3569.